Non-intrusive Measurement of Partial Discharge and its Extraction Using Short Time Fourier Transform

Guomin Luo[1], Daming Zhang[1], *Member, IEEE* and Wenghoe Leong[2]

***Abstract*— Non-intrusive measurement of partial discharge (PD) is very attractive but de-noising of the measured signal from it is an obstacle to overcome before it can be accepted as a feasible approach. In this paper, a pulse extraction method based on short time Fourier transform (STFT) is proposed and then used on some field-test PD signals by non-intrusive measurement technique. Energy spectrums in time-frequency (TF) domain of those signals are generated by STFT. Frequency bands with possible PDs are then selected. The minimax frequency-dependent threshold is applied to examine the selected frequency bands and remove the noises. Finally, the signal segments with similar energy spectrum in selected frequency bands are combined to form the extracted pulses. Compared with the wavelet thresholding method, the STFT-based method is more effective in extracting and grouping the pulses in signals with low signal-to-noise ratio (SNR). Further more STFT results in two-time-occurrence-per-cycle PD signals, which are very much the same as those observed in laboratory test. Since the field data was obtained from a power transformer under operation of more than 17 years, one has confidence to conclude that the extracted pulses are true PD signals.**

***Index Terms*—Partial discharge, pulse extraction, noise removal, time frequency analysis, short time Fourier transform.**

I. Introduction

GAS insulated switchgears or substations (GIS) are expensive and extremely important in power grid. Their reliability is crucial to the entire system. The failures of GIS due to insulation breakdown will result in serious faults and large repair cost. For this reason, the monitoring of GIS insulation level is needed to find the deteriorations at their earlier stage.

Partial discharge (PD) which is caused by the deterioration of insulation of high voltage (HV) equipment is often detected as a means of insulation evaluation. Its detection involves the capture, storage and processing of PD signals, which occur in the form of individual or series of electrical pulses[1]. But noise is always a major obstacle to obtain a solid conclusion on which measured pulse is a true PD. Because of the influence from the outer disturbance, the oscillatory wave from amplifier and so on, the PD pulses are mostly submerged in noise. Besides hardware improvement, signal processing is another powerful tool for PD extraction and classification. Both the time-domain features, such as magnitude, phase angle, numbers, and pulse waveform, and the frequency-domain features, like frequency spectrum, have been employed in PD analysis for a very long time[2],[3].

Recently, time-frequency analysis becomes more and more popular in PD analysis. Because the PD pulses have unique features in long-term-used transformers etc, such as repetitive and appearing at similar phase angles in each cycle, they reveal a different TF spectrum from other communication signals or pulse-like noises from power electronics equipments. Some papers have adopted TF tools, for example, continuous wavelet transform (CWT), Wigner-Ville distribution and Gabor transform, to explore the characteristics of PDs[4-6]. They pointed out the possibility of PD extraction with TF spectrum. But those papers only focused on PDs collected from laboratory experiments where the signal-to-noise (SNR) ratio is quite high. The noise removal in TF spectrum and the PD extraction methods, the toughest parts in practical application, have not been investigated.

In this paper, a PD extraction method with short-time Fourier transform (STFT) is proposed. First, the fundamental of STFT is introduced. Then the basic procedure of this pulse extraction method is presented in detail. The method is used on some field-test data collected from Singapore Shaw Tower. Finally, this method is compared with existing wavelet-based algorithm and its efficiency is demonstrated.

II. Fundamental of Short Time Fourier Transform

Short time Fourier transform (STFT) is also called windowed Fourier transform. It was developed from Fourier transform and has often been used to determine the sinusoidal frequency components and phase features of local sections of signal.

The Fourier analysis represents any finite energy function $f(t)$ as a sum of sinusoidal waves $e^{i\omega t}$. The amplitude of Fourier transform $\hat{f}(\omega)$ of each sinusoidal wave $e^{i\omega t}$ is equal to its correlation with f [7]:

Authors 1 are with school of electrical and electronic engineering, Nanyang Technological University, Singapore (email: edmzhang@ntu.edu.sg); Author 2 is with Hoestar Inspection International Pte Ltd.

$$\hat{f}(\omega) = \int_{-\infty}^{+\infty} f(t) e^{-i\omega t} dt \quad (1)$$

The more regular $f(t)$, the faster the decay of the sinusoidal wave amplitude $|\hat{f}(\omega)|$ when frequency ω increases. But after Fourier transform, all time-domain features of the signal are lost.

In order to keep the time-domain information, the STFT was introduced. A real and symmetric window $g(t)=g(-t)$,translated by u and modulated by the frequency ξ, is added:

$$g_{u,\xi}(t) = e^{i\xi t} g(t-u) . \quad (2)$$

It is normalized $\|g\|=1$ so that $\|g_{u,\xi}\|=1$ for any real numbers u and ξ. The resulting STFT of f is

$$Sf(u,\xi) = \langle f, g_{u,\xi} \rangle = \int_{-\infty}^{+\infty} f(t) g(t-u) e^{-i\xi t} dt \quad (3)$$

When the window $g(t)$ slides along the time axis, the frequency spectrum of the signal segment is revealed. The spectrum of the whole time range forms a two-dimensional representation of signal which is called time-frequency spectrum[8].

III. Pulse Extraction Using Time-Frequency Method

A. Basic Procedure

Since the PD pulses from the same source have similar frequency spectrum and very short intervals, a group of PD series can form a cloud-like component in TF spectrum. Extracting all the cloud-like components will help to find the locations of pulses from the same source. The implementation steps of PD pulse extraction using STFT are listed as follow:

1) Perform the time-frequency analysis of the detected signal. In order to find more exact frequency range, larger $g(t)$ window is employed, for example, 0.2 millisecond for a one-cycle (50Hz) signal.

2) Select and record the frequency bands with cloud-like components.

3) Perform the STFT again with smaller $g(t)$ window (for example, 0.02 millisecond), and extract the spectrum within the frequency bands recorded in step 2. De-noise and group the pulses.

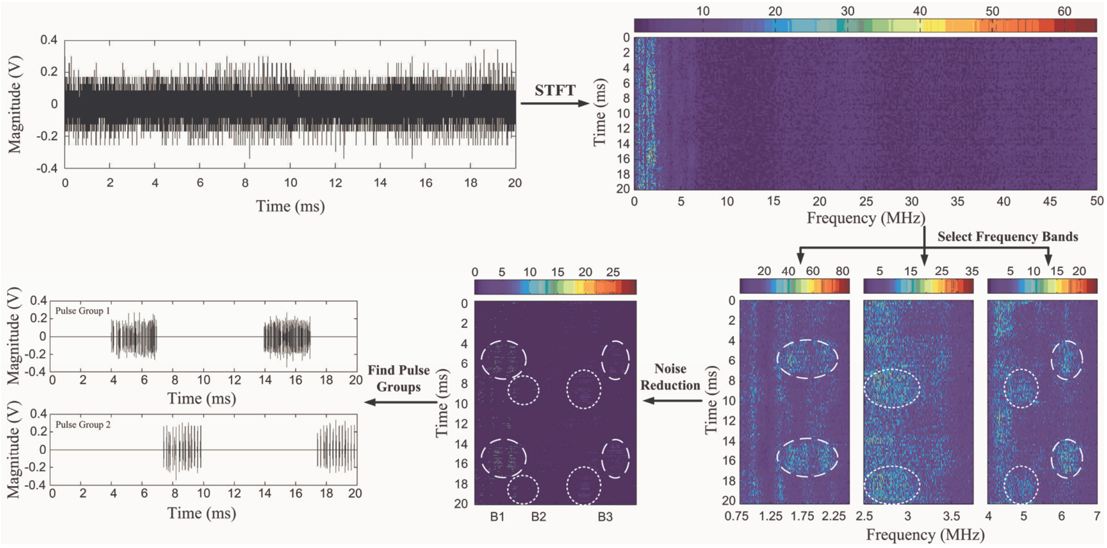

Fig. 1. Basic Procedure of pulse extraction using STFT.

4) Extract the PD pulses of the same group.

This procedure is illustrated in Fig.1 and explained in detail in following paragraphs. The data used in Fig.1 is provided by Singapore Hoestar Inspection International Pte Ltd with 2 million samples per cycle.

B. Frequency Bands Selection

It is very important to find the frequency bands that contain pulse energy. The PD pulses usually have very short duration that means a very wide frequency range. But when noises are added, especially periodic noises, the PD energy will be totally submerged in noises in some frequency bands, in which it is a tough job to find PDs. However, there are always some frequency bands that contain greater pulse energy than noises appear to be series of ‘clouds’ in the TF spectrum.

Since those cloud-like components often have small energy and their locations and numbers are uncertain, a manual selection technique is currently employed.

C. Noise Removal

The noise removal is to decide the useful part in spectrum. As the noise level in TF spectrum varies with frequency and the PD energy is small, the frequency-dependent minimax threshold is a good choice. This threshold is defined to optimize a criterion based on mean squared error (MSE). The threshold δ is demonstrated as follows:

$$\delta = \sigma * (0.3936 + 0.1829 * \log_2 N) . \quad (4)$$

where σ is the estimation of white noise. It equals the median value of the spectrum with the same frequency divided by 0.6745. N is the length of time axis of TF spectrum[9].

D. Pulses Grouping

As mentioned in step 3, STFT is performed two times in this procedure. The first TF spectrum with larger $g(t)$ window provides more information of frequency distribution. It helps the researchers to find the right frequency bands. But the larger $g(t)$ window could be troublesome if pulse location is required. Therefore, the STFT is performed again with narrower window. It is the second TF spectrum used in pulse grouping.

For each frequency, the noisy parts are removed by frequency-dependent threshold. The number and energy of remained points are used to group the pulses with similar frequency and energy distribution in TF spectrum. The de-noised spectrum is shown in Fig.1 at the middle of the second row. Here ‘B1’, ‘B2’, and ‘B3’ stand for the selected frequency bands.

IV. Transient Earth Voltage and Non-Intrusive PD Sensing

When PD occurs in transformers or GIS, there is a voltage induced on its grounded or earthed metallic enclosure. To illustrate this idea, a laboratory test is set up as shown in Figure 2, where a PD generator is placed inside a metallic enclosure.

(a) (b)

Fig. 2 PD generator placed inside a metallic enclosure: (a) enclosure with its cover open (b) enclosure with its cove close

Figure 3 shows the drawing of two developed coaxial sensors for non-intrusive PD measurement, one being protruding with inner conductor 4 extending beyond the bottom of outer conductor 3 and the other being hidden with inner conductor 4 shorter than the bottom of outer conductor 3. Their pictures are shown in Figure 5 when field test is carried out.

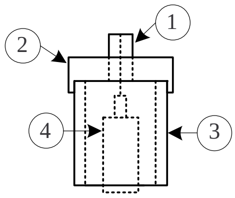

Fig. 3 Coaxial PD sensor developed for non-intrusive PD measurement, where part 1 is the female BNC interface and it is integrated with part 2

In Fig. 2(a), besides the PD generator, there is also a HFCT placed inside the metallic cavity. Using the two similar self-made sensors as shown in Fig. 3 and the HFCT, PD measurement was carried out in our laboratory. The sensor placed outside and on top of the metallic enclosure has its part 4 or inner electrode electric contact with the metallic enclosure. Similarly the sensor placed inside the metallic enclosure has its part 4 electric contact with the interior surface of the bottom of the metallic enclosure. The results are shown in Figs. 4 and 5 for two different durations, where the top wave is measured PD pulses using HFCT; the middle wave is the measured PD pulse by the sensor placed inside the enclosure; the bottom wave is output from the sensor placed outside the enclosure. From these two figures, one can see that the measured PD pulses are almost the same from the two self-made sensors placed inside and outside the metallic enclosure. Thus one can conclude that when PD occurs inside the enclosed metallic cavity, there is an induced voltage on its interior metallic surface, which is equally measurable by the sensor placed outside it. This provides fundamental basis for field test of transformers using non-intrusive self-made PD sensing technique.

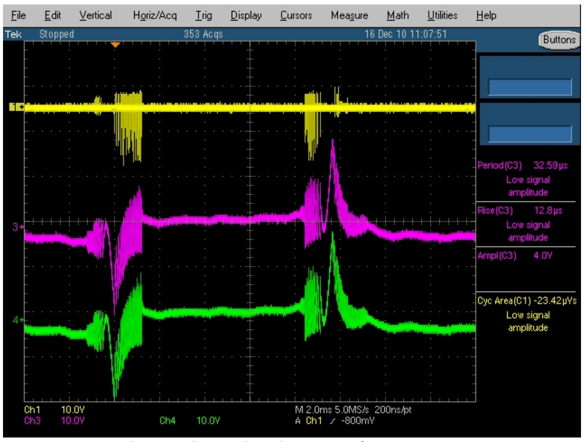

Fig. 4 Measured PD pulse with a duration of 20 ms

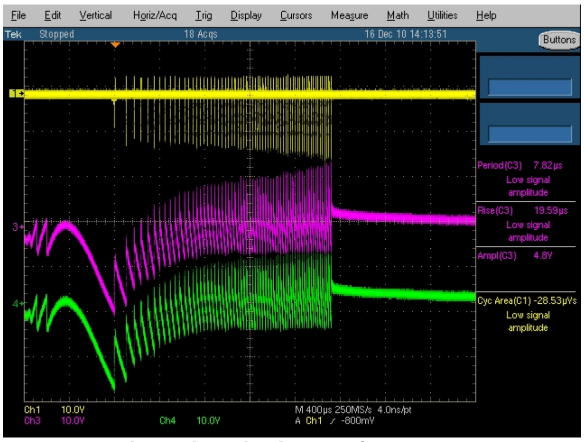

Fig. 5 Measured PD pulse with a duration of 4 ms

V. Application To Field Test

The proposed time-frequency method is used to analyze field-measured data from Singapore Shaw Tower Building. When the partial discharges happen in the transformer, a capacitive coupling of induced voltage by PD occurs between conductive part and grounded metallic shell, in a similar mechanism as described in Section IV. The data used in this paper were collected on both the cable insulation and tank wall of the transformer as shown in Fig. 6.

Fig. 6. Collection of PDs from a field transformer. (a) The sensor is attached to the cable insulation, (b) The sensors are attached on the metal tank wall.

The sensors shown in Fig. 6 are the same as those used in laboratory test.

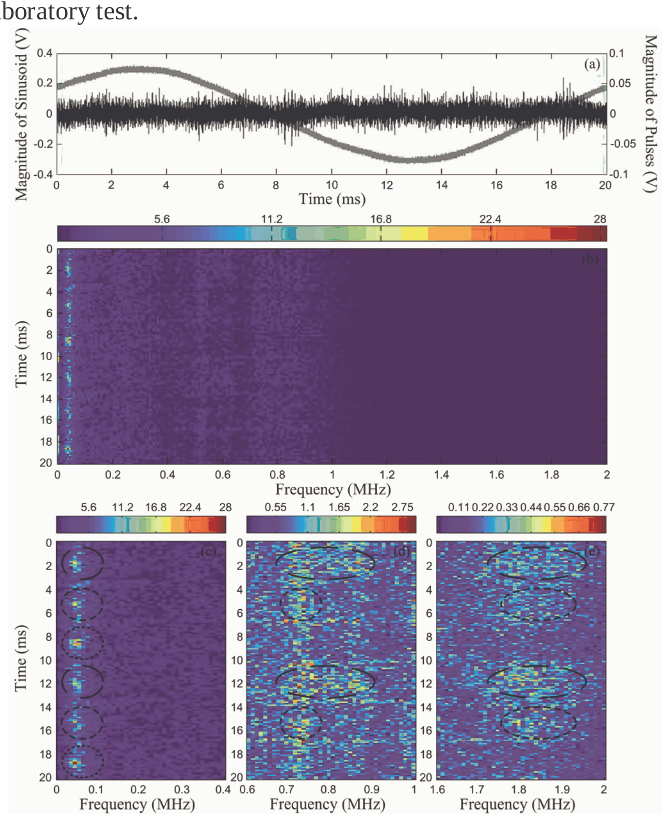

Fig. 7. Analysis of the data collected from cable insulation. (a) The original pulse data and the referencing voltage. On the left is the measurement of the sinusoidal wave. The measurement of pulses is on the other side. (b) The time-frequency spectrum of pulse signal. Figures (c) to (e) portray the selected frequency bands. (c) Band 1: frequency ranges from 0Hz to 0.4MHz, (d) Band 2: frequency ranges from 0.6MHz to 1MHz, (e) Band 3: frequency ranges from 1.6MHz to 2MHz.

A. *PD Pulses Extraction with Time-Frequency Method*

The signals collected from cable insulation and tank wall are sampled by 25MHz and 50MHz, respectively. The original data, the TF spectrum and the selected frequency bands of each signal are shown in Fig.7 and Fig.8.

In the selected frequency bands, it is easy to find the cloud-like components in the circles with same line styles have similar properties in TF domain. Following the step 3 in basic procedure, smaller $g(t)$ window is employed to perform STFT again. With the frequency bands selected before, the extracted pulses of each group are shown in Fig.9 and Fig.10. The pulse groups denoted in different line styles in selected frequency bands ((c), (d), (e) in Fig.3 and (c), (d), (e) in Fig.4) are numbered in series.

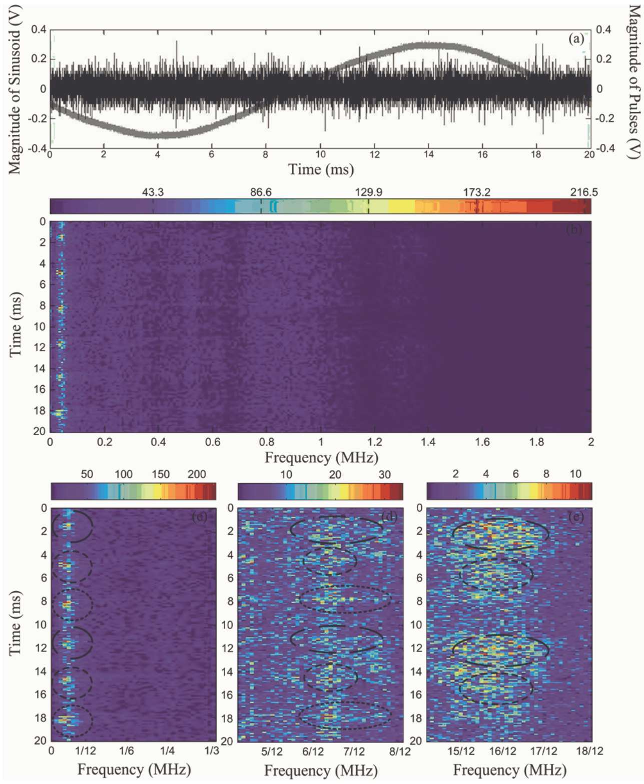

Fig. 8. Analysis of the data collected from tank wall. (a) The original pulse data and the referencing voltage. On the left is the measurement of the sinusoidal wave. The measurement of pulses is on the other side. (b) The time-frequency spectrum of pulse signal. Figures (c) to (e) portray the selected frequency bands. (c) Band 1: frequency ranges from 0Hz to 0.33MHz, (d) Band 2: frequency ranges from 0.33MHz to 0.66MHz, (e) Band 3: frequency ranges from 1.16MHz to 1.5MHz.

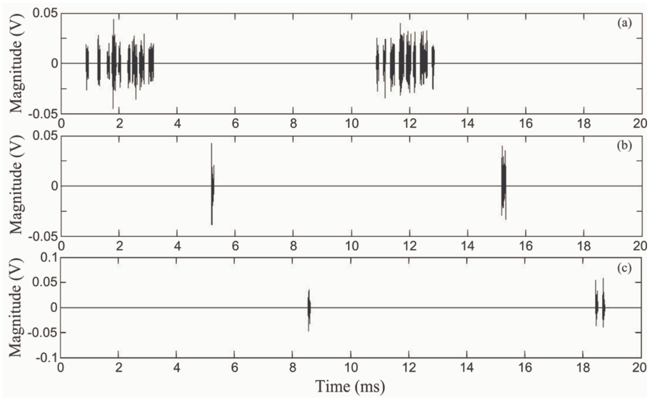

Fig. 9. Extracted pulses of signal collected from cable insulation. (a) Group 1: the 'clouds' in long dashed circles in Fig.3, (b) Group 2: the 'clouds' in short dashed circles in Fig.3, (c) Group 3: the 'clouds' in dotted circles in Fig.7.

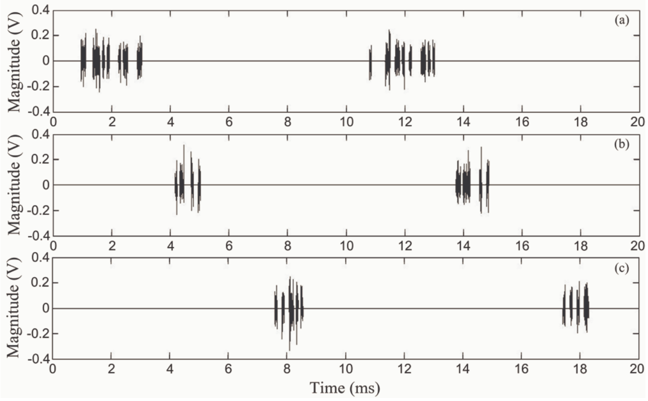

Fig. 10. Extracted pulses of signal collected from tank wall. (a) Group 1: the ‘clouds’ in long dashed circles in Fig.4, (b) Group 2: the ‘clouds’ in short dashed circles in Fig.4, (c) Group 3: the ‘clouds’ in dotted circles in Fig.8.

B. Comparison with Existing Wavelet Method

The goal of this part is to compare the performance of PD extraction of STFT-based method with another popular one, the wavelet-based algorithm. In this part multi-resolution analysis with universal level-dependent threshold as shown in [1],[11] is adopted for comparison with STFT-based method.

Unlike the STFT which can reveal all the frequency distribution of the signal segments, in multi-resolution analysis, the signal is filtered by a series of filter pairs. Each filter pair divides signal into high and low frequency bands which are also called detail part and approximate part, respectively[1]. That is to say, for a function f, the coefficients are the local average of f over neighborhoods of size proportional to 2^j, where j is decomposition scale[12]. As a typical kind of time-frequency analyzing tool, multi-resolution analysis can only divide signal into a few frequency bands, which is $j+1$. If the SNR is too low, it’s very hard for multi-resolution analysis to extract true PD pulses.

The results de-noised by wavelet-based algorithm of same signals from cable insulation and tank wall are shown in Fig.11. The decomposition scale is 6 and the wavelet base is ‘coif1’. Compared with the original signals in Fig.7(a) and Fig.8(a), the SNR of de-noised results increases. But these results still contain so much noise that it is hard to find the real PDs. In contrast, results shown in Figs. 9 and 10 clearly show two occurrences of PD pulses during one cycle. This is in very good agreement with the observation in laboratory test. In laboratory measured results as shown in Fig. 4, one can see clearly that there are two occurrences during one cycle or 20 ms, each for half a cycle. Furthermore both results measured from cable and surface of the cavity as shown in Figs. 9 and 10 follow the same conclusion drawn from laboratory measured data. Since the power transformer under test has been used for more than 17 years, periodic occurrence of PD becomes highly possible. The extracted PD signals from cable and from wall occur almost at the same phase angle with reference to power supply as shown in Figs. 7(a) and 8(a) so one can further conclude that extracted pulses in Figs. 9 and 10 are PD pulses with very high confidence level.

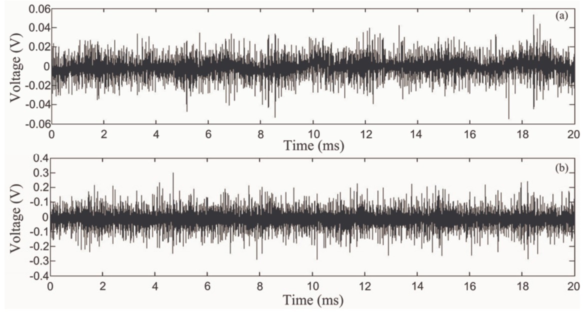

Fig. 11. De-noised results by using wavelet thresholding method. (a) The results of signal collected from cable insulation, (b) The results of signal collected from tank wall.

VI. Conclusion

In this paper, the STFT-based method has been presented as an efficient tool to extract the PD pulses in field measured signals with very low SNR. The efficiency and consistency of time-frequency analysis are demonstrated using a number of field-test data from different sensors and locations. This paper shows that this STFT-based method can more satisfactorily supersede other existing methods in PD extraction.

However, in this paper, a manual selection of frequency bands relies on the experiences of researchers or engineers. The future research work should involve the algorithm to realize automatic selection of frequency bands.

References

[1] G. M. Luo and D. M. Zhang, “Application of wavelet transform to study partial discharge in XLPE sample,” in *Proc. Power Engineering Conference, AUPEC*. Australasian Universities, 2009, pp. 1-6.

[2] R. Bartnikas and M. Pompili, “Partial discharge measurements,” *IEEE Trans. Dielectrics and Electrical Insulation*, vol. 15, pp. 1487-1487, Dec 2008.

[3] A. Ardito, R. Iorio, G. Santagostino, and A. Porrino, “Accurate modeling of capacitively graded bushings for calculation of fast transient over voltages in GIS,” *IEEE Trans. Power Delivery*, vol. 7, pp. 1316-1327, 1992.

[4] C. Caironi, D. Brie, L. Durantay, and A. Rezzoug, “Interest and utility of time frequency and time scale transforms in the partial discharges analysis,” in *Conf. Rec. 2002 IEEE Int. Symposium. Electrical Insulation*, pp. 516-522.

[5] K. L. Wong, “Electromagnetic emission based monitoring technique for polymer ZnO surge arresters,” *IEEE Trans. Dielectrics and Electrical Insulation*, vol. 13, pp. 181-190, 2006.

[6] Z. Jia, Y. Hao, and H. Xie, “The degradation assessment of epoxy/mica insulation under multi-stresses aging,” *IEEE Trans. Dielectrics and Electrical Insulation*, vol. 13, pp. 415-422, 2006.

[7] S. G. Mallat, *A Wavelet Tour of Signal Processing: The Sparse Way*. Amsterdam, Boston: Elsevier/Academic Press, 2009, p. 2.

[8] S. G. Mallat, *A Wavelet Tour of Signal Processing: The Sparse Way*, Amsterdam, Boston: Elsevier/Academic Press, 2009, pp. 92-93.

[9] D. L. Donoho and I. M. Johnstone, “Threshold selection for wavelet shrinkage of noisy data,” in *Proc. 16th Annu. Int. Conf. Engineering in Medicine and Biology Society*, USA, 1994, pp. A24-A25 vol.1.

[10] Y. Li, Y. Wang, G. Lu, J. Wang, and J. Xiong, “Simulation of transient earth voltages aroused by partial discharge in switchgears,” in *Proc. Int. Conf. High Voltage Engineering and Application (ICHVE)*, 2010, pp. 309-312.

[11] X. Ma, C. Zhou, and I. J. Kemp, “Interpretation of Wavelet Analysis And Its Application In Partial Discharge Detection,” *IEEE Trans. Dielectrics and Electrical Insulation*, vol. 9, pp. 446-457, 2002.

[12] S. G. Mallat, *A Wavelet Tour of Signal Processing: The Sparse Way*, Amsterdam, Boston: Elsevier/Academic Press, 2009, p. 264.